15(S)-HETE Production in Human Retinal Microvascular Endothelial Cells by Hypoxia: Novel Role for MEK1 in 15(S)-HETE–Induced Angiogenesis

Arun K. Bajpai,[1] *Eva Blaskova,*[1] *Suresh B. Pakala,*[1] *Tieqiang Zhao,*[1] *Wayne C. Glasgow,*[2] *John S. Penn,*[3] *Dianna A. Johnson,*[4] *and Gadiparthi N. Rao*[1]

Purpose. To examine for the expression of 15-lipoxygenase 1 (15-LOX1) and 15-LOX2 in human retinal microvascular endothelial cells (HRMVECs) and study the role of arachidonic acid metabolites of these enzymes in angiogenesis.

Methods. Quantitative RT-PCR and reverse-phase HPLC analyses were used to determine 15-LOX1/2 expression and their arachidonic acid metabolites in HRMVECs. The role of MEK1 in 15(S)-HETE–induced angiogenesis was studied using HRMVEC migration, tube formation, and basement membrane matrix plug angiogenesis.

Results. HRMVECs expressed both 15-LOX1 and 15-LOX2. Hypoxia induced the expression of 15-LOX1 and the production of its arachidonic acid metabolites 15(S)-hydroxyeicosatetraenoic acid (15(S)-HETE) and 12(S)-hydroxyeicosatetraenoic acid (12(S)-HETE). 15(S)-HETE stimulated HRMVEC migration and tube formation as potently as 20 ng/mL fibroblast growth factor-2 (FGF-2). In addition, 15(S)-HETE stimulated the phosphorylation of ERK1/2, JNK1, p38 MAPK, and MEK1 in a time-dependent manner in these cells. Inhibition of MEK1 by pharmacologic and dominant-negative mutant approaches attenuated 15(S)-HETE–induced phosphorylation of ERK1/2 and JNK1 but not p38 MAPK. Blockade of ERK1/2 and JNK1 activation suppressed 15(S)-HETE–induced HRMVEC migration and tube formation and basement membrane matrix plug angiogenesis. Inhibition of p38 MAPK attenuated 15(S)-HETE–induced HRMVEC migration only. Inhibition of MEK1 also blocked 15(S)-HETE–induced HRMVEC migration and tube formation and basement membrane matrix plug angiogenesis.

Conclusions. These results suggest that hypoxia, through the induction of 15-LOX1 expression, leads to the production of 15(S)-HETE in HRMVECs. In addition, 15(S)-HETE, through MEK1-dependent activation of ERK1/2 and JNK1, stimulates the angiogenic differentiation of HRMVECs and basement membrane matrix plug angiogenesis. (*Invest Ophthalmol Vis Sci.* 2007;48:4930–4938) DOI:10.1167/iovs.07-0617

From the Departments of [1]Physiology and [4]Ophthalmology, University of Tennessee Health Science Center, Memphis, Tennessee; [2]Division of Basic Medical Sciences, Mercer University School of Medicine, Macon, Georgia; and [3]Vanderbilt Eye Institute, Vanderbilt University School of Medicine, Nashville, Tennessee.

Supported by National Eye Institute/National Institutes of Health Grant EY014856.

Submitted for publication May 24, 2007; revised July 3, 2007; accepted September 12, 2007.

Disclosure: **A.K. Bajpai**, None; **E. Blaskova**, None; **S.B. Pakala**, None; **T. Zhao**, None; **W.C. Glasgow**, None; **J.S. Penn**, None; **D.A. Johnson**, None; **G.N. Rao**, None

The publication costs of this article were defrayed in part by page charge payment. This article must therefore be marked "*advertisement*" in accordance with 18 U.S.C. §1734 solely to indicate this fact.

Corresponding author: Gadiparthi N. Rao, Department of Physiology, University of Tennessee Health Science Center, 894 Union Avenue, Memphis, TN 38163; grao@physio1.utmem.edu.

In addition to its prominent role in normal development and wound healing,[1,2] angiogenesis plays an important role in the progression of several diseases, including atherosclerosis, cancer, and diabetic retinopathy.[3–7] In particular, angiogenesis appears to be a critical factor in proliferative vitreoretinal diseases such as proliferative vitreoretinopathy (PVR) and proliferative diabetic retinopathy (PDR).[6,7] Under hypoxic conditions, several metabolic consequences may take place, including the cessation of oxidative phosphorylation. As a result, the tissues experiencing hypoxia switch to anaerobic metabolism for their energy needs. When the use of ATP becomes greater than its production, adenosine accumulates.[8,9] Similarly, impairment in the blood supply results in the accumulation of metabolic products such as lactate and CO_2 in the interstitial space. Although some of these metabolites dilate blood vessels and thus increase the blood supply to the affected regions in an acute manner,[10,11] under sustained hypoxic conditions they may also act as angiogenic factors.[9] As an adaptive response to low-oxygen tension, the endothelial cells may produce a variety of growth factors, including vascular endothelial growth factor (VEGF),[12] fibroblast growth factor-2 (FGF-2),[13] insulin-like growth factor-1 (IGF-1),[14] and platelet-derived growth factor (PDGF),[15] to stimulate their own growth and new blood vessel formation in the surrounding area. Among these factors, VEGF is the most potent in stimulating angiogenesis in retina under hypoxic conditions.[6]

A large body of data indicates that lipoxygenases play a role in the pathogenesis of various diseases, including cancer and atherosclerosis.[16–19] In delineating the mechanisms underlying the involvement of lipoxygenases in these disease processes, it was reported that 12(S)-hydroxyeicosatetraenoic acid (12(S)-HETE), the 12-lipoxygenase (12-LOX) product of arachidonic acid, influences the growth and motility of cancer cells and vascular smooth muscle cells.[20,21] Similarly, 12(S)-HETE has been shown to stimulate angiogenesis.[22] In regard to the role of other lipoxygenases in the pathogenesis of these diseases, it was reported that 15-LOX1, while inhibiting colorectal cancer cell growth,[23,24] stimulates prostate cancer cell growth.[17,18,25] In contrast, 15-LOX2 has been shown to inhibit prostate cancer growth.[26] Although 15-LOX1 preferentially converts linoleic acid to 13(S)-hydroxy octadecadienoic acid (13(S)-HODE), it also metabolizes arachidonic acid to 15(S)-HETE and 12(S)-HETE.[27] On the other hand, 15-LOX2 converts arachidonic acid exclusively to 15(S)-HETE.[27] In regard to the actions of 15-LOX1/2 metabolites of arachidonic acid/linoleic acid in these cells, only 13(S)-HODE mimicked the effects of 15-LOX1 on the inhibition of colorectal cancer cell growth.[23,24] On the other hand, 15(S)-HETE exhibited proangiogenic activity in endothelial cells[28] and enhanced the growth of some cancer cell types such as erythroid cells.[16] Thus, 15-LOX1/2 and its products, 13(S)-HODE and 15(S)-HETE, exhibited differential effects in different cancer cell types. In addition to these observations, it was reported that on exposure to hypoxia, human neonatal vessels produce levels of 15(S)-HETE higher than normoxic levels.[29]

Because 15(S)-HETE induced growth in some cancer cell types and its production was increased in hypoxia-exposed neonatal vessels, we sought to determine whether this eicosanoid stimulates neovascularization and thereby contributes to the pathogenesis of PDR. In the present study we showed that hypoxia induces the expression of 15-LOX1 and the production of its arachidonic acid metabolites 15(S)-HETE and 12(S)-HETE. In addition, 15(S)-HETE through MEK1-dependent activation of ERK1/2 and JNK1 induced the angiogenic differentiation of HRMVEC and basement membrane matrix (Matrigel; BD Biosciences, Bedford, MA) plug angiogenesis.

Materials and Methods

Reagents

Aprotinin, dithiothreitol, HEPES, leupeptin, phenylmethylsulfonyl fluoride (PMSF), sodium deoxycholate, and sodium orthovanadate were purchased from Sigma Chemical Company (St. Louis, MO). Nordihydroguaiaretic acid (NDGA) was obtained from Aldrich Chemical Company (Milwaukee, WI). Anti–leukocyte 12-LOX antibodies (catalog no. 160304), 5(S)-HETE, 12(S)-HETE, and 15(S)-HETE were bought from Cayman Chemicals (Ann Arbor, MI). Growth factor-reduced basement membrane matrix (Matrigel; catalog no. 354250) was obtained from BD Biosciences (Bedford, MA). Phosphospecific anti-ERK1/2 (catalog no. 9101), anti-JNK1 (catalog no. 9251), anti-p38 MAPK (catalog no. 9216), and anti-MEK1/2 (catalog no. 9121) antibodies were bought from Cell Signaling Technology (Beverly, MA). Anti-ERK2 (catalog no. SC-154), anti-JNK1 (catalog no. SC-474), anti-MEK1 (catalog no. SC-219), anti-p38 MAPK (catalog no. SC-535), and anti–β-tubulin (catalog no. SC-9104) antibodies were obtained from Santa Cruz Biotechnology, Inc (Santa Cruz, CA). Anti–15-LOX2 antibodies were bought from Oxford Biomedical Research (Oxford, MI). PD98059 (catalog no. 513000), SP600125 (catalog no. 420119), and SB203580 (catalog no. 559389) were procured from Calbiochem Chemicals (San Diego, CA). [^{3}H]-Arachidonic acid (S.A. 60 Ci/mmol) was obtained from Perkin Elmer (Boston, MA). All the primers were made by IDT (Coralville, IA). All experiments were performed in accordance with the ARVO Statement for the Use of Animals in Ophthalmic and Vision Research and were approved by the Animal Care and Use Committee of the University of Tennessee Health Science Center (Memphis, TN).

Construction of Adenoviral Vectors

The human dnMEK1 cDNA fragment was released from pMCL-hMMK1-K97M by digestion with *Kpn*I and *Hin*dIII[30] and were cloned into the same sites of pBluescript II SK (+) vector. The human dnMEK1 cDNA was then cloned into *Kpn*I and *Not*I sites of entry vector pENTR3C after its release from the pBluescript II SK (+) plasmid by digestion with the same restriction enzymes. The pAd-dnMEK1 construct was obtained by recombination between pdnMEK1-ENTR3C and pAdCMVV5DEST (Invitrogen, Carlsbad, CA) and was verified by DNA sequencing. The construction of pAd-GFP was described previously.[31] pAd-GFP and pAd-dnMEK1 were linearized with *Pac*I and transfected into HEK293A cells. The resultant adenovirus was further amplified by infection of HEK293A cells and was purified by cesium chloride gradient ultracentrifugation.[32]

Cell Culture

Human retinal microvascular endothelial cells (HRMVECs; catalog no. ACBRI 181) were purchased from Applied Cell Biology Research Institute (Kirkland, WA). Human dermal microvascular endothelial cells (HDMVECs; catalog no. C-011–5C) were purchased from Cascade Biologics (Portland, OR). Cells were grown in medium 131 containing microvascular growth supplements (MVGS), 10 μg/mL gentamicin, and 0.25 μg/mL amphotericin B. Cultures were maintained at 37°C in a humidified 95% air/5% CO_2 atmosphere. Cells underwent quiescence by incubation in medium 131 for 24 hours and were used for the experiments unless otherwise indicated.

Hypoxia

To achieve hypoxia (1% O_2), a preanalyzed air mixture (5% CO_2/95% N_2) was infused into airtight chamber-containing cells (Billups-Rothen-

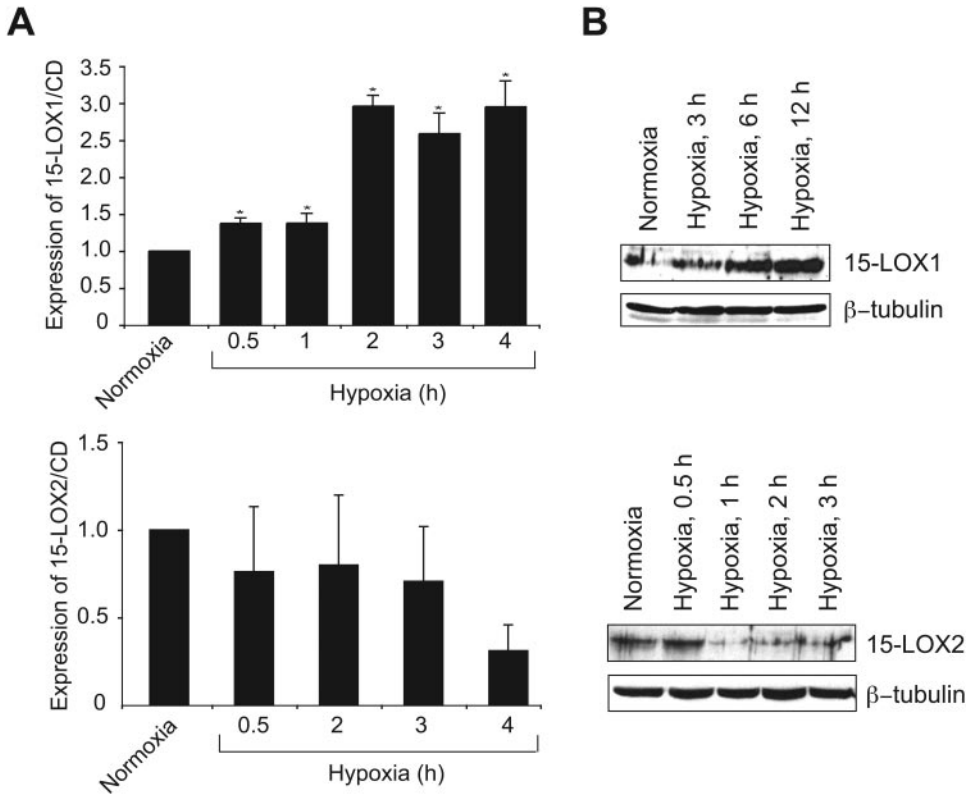

Figure 1. Differential regulation of 15-LOX1 and 15-LOX2 in HRMVECs by hypoxia. (**A**) An equal amount of total cellular RNA from control and various time points of hypoxia-treated HRMVECs was analyzed for 15-LOX1 and 15-LOX2 mRNA levels by qRT-PCR. (**B**) An equal amount of protein from control and various time points of hypoxia-treated HRMVECs was analyzed by Western blotting for 15-LOX1 and 15-LOX2 protein levels using their specific antibodies. Values are the mean ± SD of three independent experiments. * $P < 0.01$ versus control.

berg Inc., Delmar, CA) at a flow rate of 3 L/min per 15 minutes. The hypoxic chamber was then placed in a tissue culture incubator at 37°C for the desired length of time.

Reverse- and Chiral-Phase HPLC Analyses of Arachidonic Acid Metabolites

HRMVECs labeled with [^{3}H]-arachidonic acid (0.5 μCi/mL), after quiescence in medium 131, were subjected to hypoxia for the indicated times. The eicosanoids released into the medium were extracted in methanol at a final concentration of 10% (vol/vol). The cell monolayer was rinsed with methanol, and the rinse was added to this mixture. The pH of the mixture was adjusted to 2.5 with 10% (vol/vol) glacial acetic acid, and it was then passed through a solid-phase extraction column (Pre-Sep C18; J. T. Baker, Phillipsburg, NJ). Arachidonic acid metabolites were eluted with 100% methanol followed by evaporation to dryness. The metabolites were reconstituted in 50 μL of 100% methanol and were analyzed by reverse-phase high-performance liquid chromatography using C18 column (5-μm particle size, 4.6 × 250 mm; Beckman Instruments, Berkeley, CA), as described, using methanol/water/acetic acid with 55:45:0.01 and 75:25:0.01 ratios and 100% methanol as mobile phases at a flow rate of 1.0 mL/min for 40 minutes, 30 minutes, and 20 minutes, respectively.[33,34] For identification of the racemic state of 15-HETE, cells were incubated with 10 μCi [^{3}H]-arachidonic acid under hypoxia at 37°C for 30 minutes, and the eicosanoids released into the medium were extracted and analyzed by reverse-phase HPLC. The 15-HETE fractions were collected and subjected to chiral-phase HPLC (Whelk-O1 column) with 4-(3,5-dinitrobenzamido) tetrahydrophenanthrene as a stationary phase and hexane/isopropanol/acetic acid (100:1.5:0.1) as a mobile phase. One-milliliter fractions were collected, and the radioactivity in the fractions was

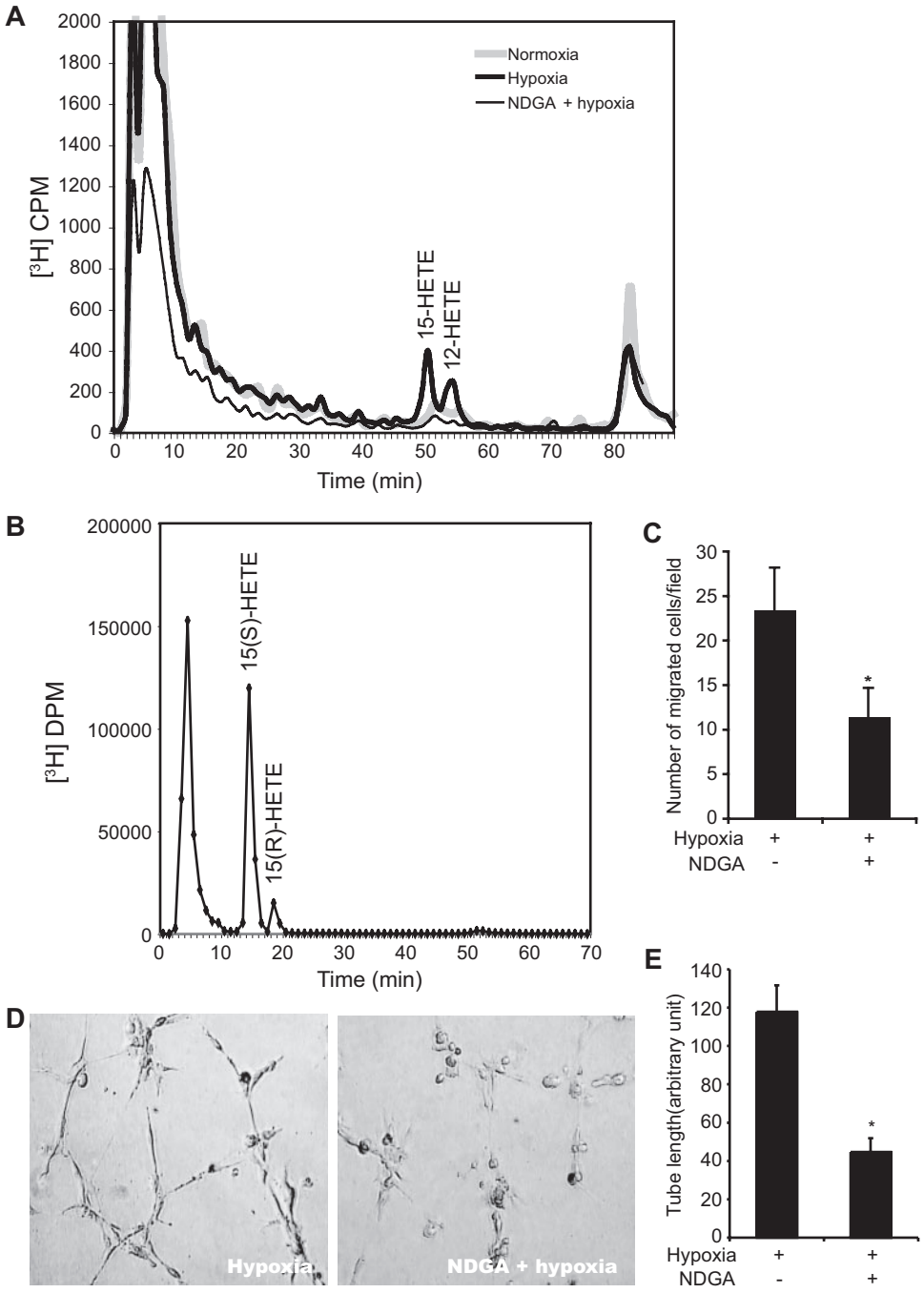

FIGURE 2. Hypoxia induced the production of 15(S)-HETE and 12(S)-HETE in HRMVECs. (**A**) HRMVECs that were prelabeled with [^{3}H]-AA and that underwent quiescence were kept at normoxia or subjected to hypoxia for 6 hours in the presence and absence of NDGA (25 μM), a potent inhibitor of LOX. At the end of the incubation period, the eicosanoids released into the culture medium were extracted and analyzed by reverse-phase HPLC. (**B**) All the conditions were the same as (**A**) except that cells were subjected to hypoxia for 30 minutes in the presence of 10 μCi [^{3}H]-arachidonic acid and 10 μM calcium ionophore A23187. After separation by reverse-phase HPLC, 15-HETE fractions were collected and subjected to chiral-phase HPLC. (**C**) HRMVEC migration was measured using modified Boyden chambers under hypoxia in the presence and absence of 25 μM NDGA. (**D**, **E**) HRMVEC tube formation was measured in growth factor–reduced basement membrane matrix–coated 24-well plates under hypoxia in the presence and absence of 25 μM NDGA. Representative tube formation (**D**) and quantitative data (**E**). Values are the mean ± SD of three independent experiments. $^*P < 0.01$ versus hypoxia treatment alone.

determined by mixing them with full spectrum fluorescent light (Ecolume; Lumiram, Larchmont, NY) scintillation fluid and counting in a liquid scintillation counter.

Real-Time Quantitative RT-PCR

Total RNA was isolated from control and hypoxia-treated HRMVECs using TRIzol reagent according to the manufacturer's protocol (Sigma Chemical, St. Louis, MO). To carry out the real-time quantitative RT-PCR (qRT-PCR) amplification of 15-LOX-1 and 15-LOX-2, cDNA was generated with 1 μg RNA from control and hypoxia-treated HRMVECs using a cDNA RT kit (High-Capacity cDNA Reverse Transcription; catalog no. 4368814; Applied Biosystems, Foster City, CA). Complementary DNA synthesis was performed in 0.2-mL PCR tubes consisting of 100 μL of the following reaction mixture: 1 μg RNA, 10 μL 10× random primers, 4 μL 25× dNTPs (100 mM), 5 μL reverse transcriptase (50 U/μL), and 10 μL RT buffer; the rest was RNase-free H_2O.

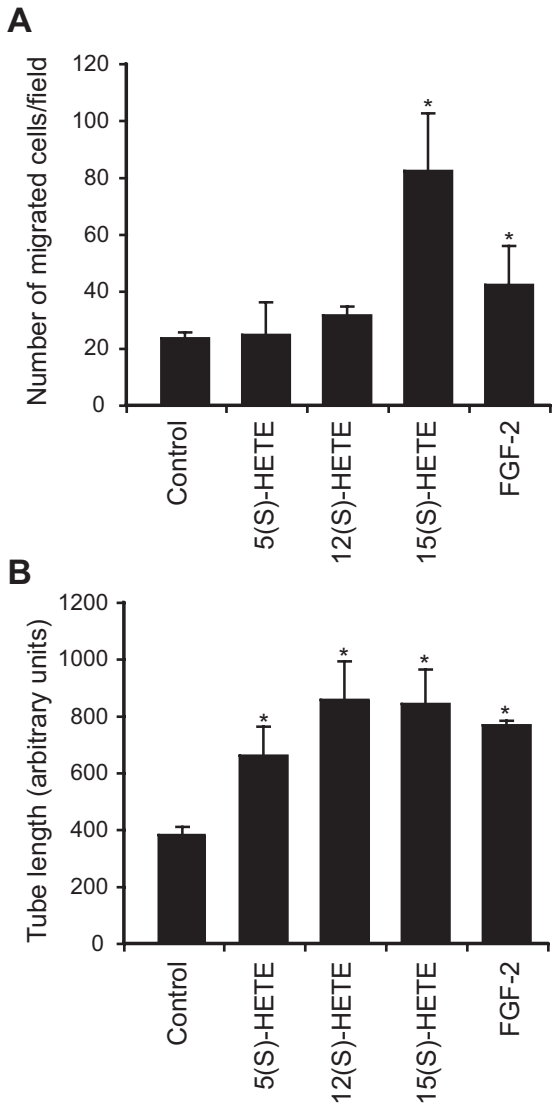

FIGURE 3. Effects of 5(S)-HETE, 12(S)-HETE, 15(S)-HETE, and FGF-2 on HRMVEC migration and tube formation. (**A**) HRMVEC migration in response to vehicle or 0.1 μM of the indicated HETE or 20 ng/mL of FGF-2 was measured by modified Boyden chamber method. (**B**) HRMVEC tube formation in response to vehicle or 0.1 μM of the indicated HETE or 20 ng/mL of FGF-2 was measured in growth factor–reduced basement membrane matrix–coated 24-well plates. Values are the mean ± SD of three independent experiments. $^*P < 0.01$ versus control.

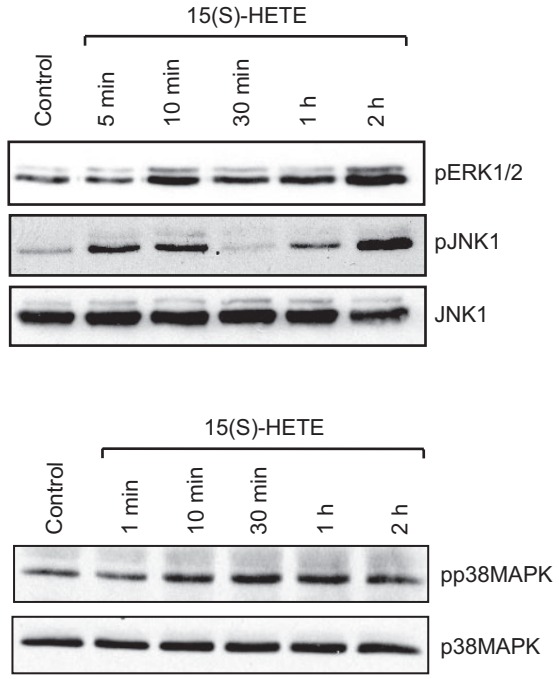

FIGURE 4. 15(S)-HETE stimulates phosphorylation of ERK1/2, JNK1, and p38 MAPK in a time-dependent manner in HRMVECs. Quiescent HRMVECs were treated with vehicle or 0.1 μM 15(S)-HETE for the indicated times, and cell extracts were prepared. An equal amount of protein from control and each treatment was analyzed by Western blotting for phosphorylated ERK1/2, JNK1, and p38 MAPK levels using their phosphospecific antibodies. As a loading control, the blots were reprobed with anti–JNK1 or anti–p38 MAPK antibodies.

Messenger RNA copy numbers for 15-LOX1, 15-LOX2, and cyclophilin D were determined by qRT-PCR using a fluorescence temperature rapid-air cycle (Light Cycler 480; Roche Applied Science, Indianapolis, IN). Amplifications were performed in a 10-μL reaction mixture containing 2 μL cDNA solution, 0.1 μL Universal Library Probe (10 μM), 0.1 μL forward primer (20 μM), 0.1 μL reverse primer (20 μM), 5 μL LC 480 master mix (2×), and 2.7 μL H_2O. Standard curves were generated for each assay run. All primers for real-time qRT-PCR assays spanned at least one intron, so that any containing DNA did not contribute to the amplifier on which quantification was based. The primers for 15-LOX1 were 5′-AGC CTG ATG GGA AAC TCT TG-3′ (forward) and 5′-AGG TGG TGG GGA TCC TGT-3′ (reverse), which gave a 68-nt amplified product. The primers for 15-LOX2 were 5′-GAT CTT CAA CTT CCG GAG GAC-3′ (forward) and 5′-ACT GGG AGG CGA AGA AGG-3′ (reverse), which gave an 80-nt amplified product. The primers for cyclophilin D were 5′-GGA GAC TTC TCA AAT CAG AAT GG-3′ (forward) and 5′-ACC CTC CCG ATC ATG CTT-3′ (reverse), which gave an amplified product of 96 nt. UPL probes number 42 with sequence 5′-CATCCAGC-3′ (catalog no. 04688015001), number 51 with sequence 5′- CCCAGCAG-3′ (catalog no. 04688481001), and number 39 with sequence 5′-AGGTGGAG-3′ (catalog no. 04687973001) were used as internal standard probes for monitoring the amplification of 15-LOX1, 15-LOX2, and cyclophilin D, respectively. Real-time qRT-PCR consisted of 50 cycles with the following steps: denaturation at 95°C for 30 seconds, annealing at 60°C for 30 seconds, and extension 72°C for 30 seconds. The abundance of 15-LOX1 and 15-LOX 2 was expressed relative to the cyclophilin D levels.

Cell Migration Assay

Cell migration was performed using a modified Boyden chamber method, as described by Nagata et al.[35] Cell culture inserts containing membranes with 10-mm diameter and 8-μm pore size (Nalgene Nunc International, Rochester, NY) were placed in a 24-well tissue culture

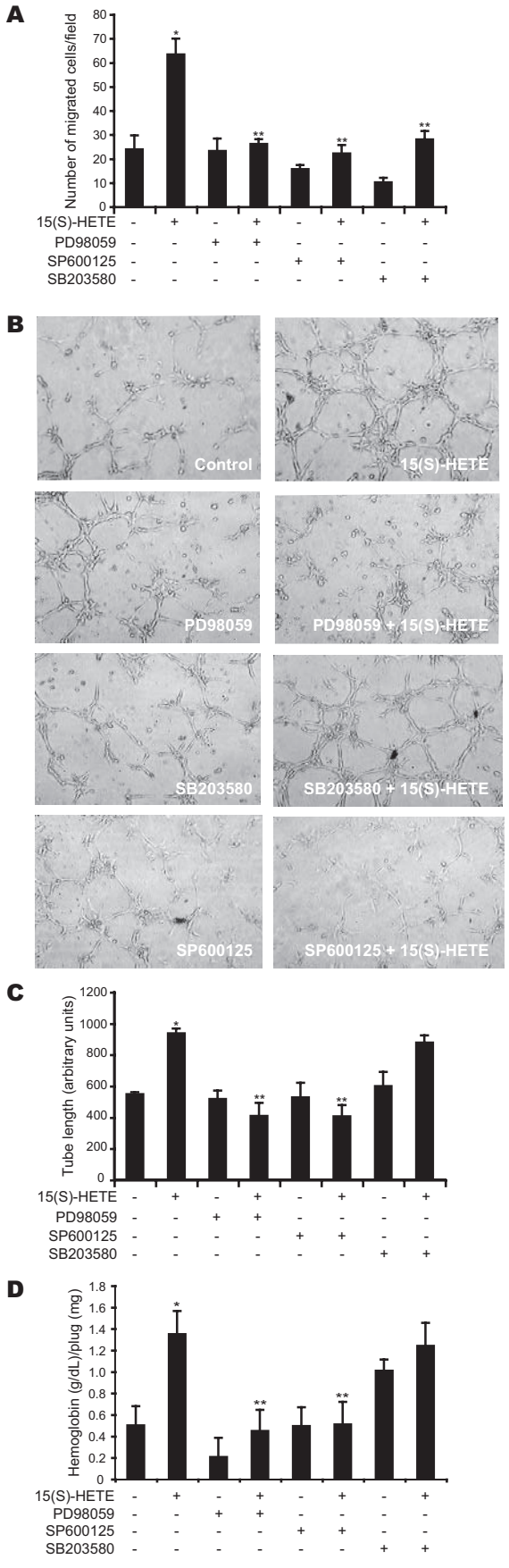

plate (Costar; Corning Incorporated, Corning, NY). The lower surface of the porous membrane was coated with 0.5% gelatin at 4°C overnight and then blocked with 0.1% heat-inactivated BSA at 37°C for 1 hour. HRMVECs underwent quiescence for 24 hours in medium 131, trypsinized, and neutralized with trypsin neutralizer solution. Cells were seeded onto the upper chamber at 1×10^5 cells/well. Vehicle or eicosanoid of interest was added to the lower chamber at the indicated concentration. Both the upper and the lower chambers contained medium 131. When the effect of dominant-negative MEK1 was tested on 15(S)-HETE–induced HRMVEC migration, cells were infected first with either Ad-GFP or Ad-dnMEK1 at a multiplicity of infection (MOI) of 80 and underwent quiescence before they were subjected to migration assay. After 8 hours of incubation at 37°C, nonmigrated cells were removed from the upper side of the membrane with cotton swabs, and the cells on the lower surface of the membrane were fixed in methanol for 15 minutes. The membrane was then stained with hematoxylin for 10 minutes and was washed once each with 50% and 100% ethanol. Cells were counted in five randomly selected squares per well under a light microscope (Eclipse 50i; Nikon, Tokyo, Japan) and were presented as number of migrated cells per field.

Tube Formation Assay

Tube formation assay was performed as described by Nagata et al.[35] Twenty-four-well culture plates (Costar; Corning Incorporated) were coated with growth factor-reduced basement membrane matrix (Matrigel; BD Biosciences) in a total volume of 280 μL/well and were allowed to solidify for 30 minutes at 37°C. HRMVECs were trypsinized, neutralized with trypsin neutralizer solution, and resuspended at 1×10^5/mL, and 200 μL of this cell suspension was added to each well. Vehicle or eicosanoid of interest, at the indicated concentration, was added to the appropriate well, and the cells were incubated at 37°C for 6 hours. When the effect of dnMEK1 was tested on 15(S)-HETE–induced HRMVEC tube formation, cells were infected first with either Ad-GFP or Ad-dnMEK1 at an MOI of 80 and then underwent quiescence before they were subjected to tube formation. Tube formation was observed under an inverted microscope (Eclipse TS100; Nikon). Images were captured with a charge-coupled device color camera (KP-D20AU; Hitachi, Honshu, Japan) attached to the microscope, and the tube length was measured using the National Institutes of Health Image J 1.31 v Program.

Western Blot Analysis

After appropriate treatments, HRMVECs were rinsed with cold phosphate-buffered saline (PBS) and lysed in 500 μL lysis buffer (PBS, 1% Nonidet P-40, 0.5% sodium deoxycholate, 0.1% SDS, 100 μg/mL PMSF, 100 μg/mL aprotinin, 1 μg/mL leupeptin, and 1 mM sodium orthovanadate) on ice for 20 minutes. Cell lysates were scraped into 1.5-mL

FIGURE 5. Effect of blockade of ERK1/2, JNK1, and p38 MAPK on 15(S)-HETE–induced HRMVEC migration and tube formation and basement membrane matrix plug angiogenesis. (**A**) HRMVEC migration in response to vehicle or 0.1 μM 15(S)-HETE in the presence and absence of PD98059 (30 μM), SP600125 (10 μM), or SB203580 (10 μM) was measured by the modified Boyden chamber method. (**B**, **C**) HRMVEC tube formation in response to vehicle or 0.1 μM 15(S)-HETE in the presence and absence of PD98059 (30 μM), SP600125 (10 μM), or SB203580 (10 μM) was measured in growth factor–reduced basement membrane matrix–coated 24-well plate. Representative tube formation (**B**) and quantification data (**C**). (**D**) C57BL/6 mice were injected subcutaneously with 0.5 mL basement membrane matrix premixed with vehicle or 50 μM 15(S)-HETE, with and without PD98059 (50 μM), SP600125 (50 μM), or SB203580 (50 μM). Seven days later, the animals were killed, and the basement membrane matrix plugs were harvested from under the skin and analyzed for hemoglobin with Drabkin reagent. Values are the mean ± SD of three independent experiments or four animals. $^*P < 0.01$ versus control. $^{**}P < 0.01$ versus 15(S)-HETE treatment alone.

Eppendorf tubes and cleared by centrifugation at 12,000 rpm for 20 minutes at 4°C. Cell lysates containing equal amounts of protein were resolved by electrophoresis on 0.1% SDS and 10% polyacrylamide gels. Proteins were transferred electrophoretically to a nitrocellulose membrane (Hybond; Amersham Pharmacia Biotech, Piscataway, NJ). After blocking in 10 mM Tris-HCl buffer, pH 8.0, containing 150 mM sodium chloride, 0.1% Tween 20, and 5% (wt/vol) nonfat dry milk, the membrane was treated with appropriate primary antibodies followed by incubation with horseradish peroxidase (HRP)-conjugated secondary antibodies. Antigen-antibody complexes were detected using chemiluminescence reagent kit (GE Health Sciences, Piscataway, NJ).

Basement Membrane Matrix Plug Angiogenesis Assay

Basement membrane matrix (Matrigel; BD Biosciences) plug assay was performed essentially as described by Medhora et al.[36] C57BL/6 male mice (8 weeks old) were lightly anesthetized with sodium pentobarbital (50 mg/kg, administered intraperitoneally) and were injected subcutaneously with 0.5 mL basement membrane matrix (Matrigel; BD Biosciences) premixed with vehicle or 50 μM of 15(S)-HETE along the dorsal midline. The injection was made rapidly with a Becton-Dickinson 26-gauge half-inch needle to ensure the entire content was delivered as a single plug. Whenever the effects of pharmacologic inhibitors, Ad-GFP or Ad-dnMKK1 were tested on 15(S)-HETE–induced angiogenesis, they were added to the basement membrane matrix (Matrigel; Becton-Dickinson) before they were injected into mice. The mice were allowed to recover, and 7 days later, unless otherwise stated, the animals were killed by inhalation of CO_2, and the basement membrane matrix (Matrigel; Becton-Dickinson) plugs were harvested from under the skin. The plugs were homogenized in 1 mL deionized H_2O on ice and cleared by centrifugation at 10,000 rpm for 6 minutes at 4°C. The supernatant was collected and used in duplicate to measure hemoglobin content with Drabkin reagent along with hemoglobin standard essentially according to the manufacturer's protocol (Sigma Chemical). Absorbance was read at 540 nm in an ELISA plate reader (Spectra Max 190; Molecular Devices, Eugene, OR). Each group contained four to six mice, and the values were expressed as gram per deciliter hemoglobin per milligram plug.

Statistical Analysis

All experiments were repeated three times with a similar pattern of results. Data are presented as mean ± SD. Treatment effects were analyzed by Student's *t*-test, and $P < 0.05$ was considered statistically significant. In the case of HPLC analysis, RT-PCR, and Western blotting, one representative set of data is shown.

Results

To understand the role of eicosanoids, particularly 15(S)-HETE, in retinal neovascularization, we first studied the effect of hypoxia on the expression of 15-LOX1/2 using qRT-PCR. Hypoxia induced a time-dependent increase in the expression of 15-LOX1 mRNA and a time-dependent decrease in the expression of 15-LOX2 mRNA (Fig. 1A). To obtain additional evidence for the effect of hypoxia on the expression of 15-LOX1/2, we also measured their protein levels. Western blot analysis of an equal amount of protein from control and various time points of hypoxia-treated HRMVEC using 15-LOX1– and 15-LOX2–specific antibodies showed a time-dependent increase in the levels of 15-LOX1 and a time-dependent decrease in the levels of 15-LOX2 in response to hypoxia (Fig. 1B). 15-LOX1 converts AA to 15(S)-HETE and 12(S)-HETE in a 3:1 ratio. On the other hand, 15-LOX2 metabolizes AA exclusively to 15(S)-HETE.[27] To determine whether hypoxia-induced expression of 15-LOX1 correlates with the production of 15(S)-HETE and 12(S)-HETE, HRMVECs were prelabeled with [^{3}H]-AA, subjected to quiescence for 24 hour, and subjected to hypoxia for 6 hours in the presence and absence of NDGA, a potent inhibitor of LOXs.[37] The eicosanoids released into the medium were extracted and analyzed by reverse-phase HPLC. Hypoxia induced the production of 15-HETE and 12-HETE in an approximately 2:1 ratio in HRMVECs. NDGA, at a concentration of 25 μM, completely suppressed their production (Fig. 2A). Although 15(S)-HETE/12(S)-HETE is formed by enzymatic actions of 15-LOX1/2 on AA, 15(R)-HETE is formed by nonenzymatic conversion of AA. Therefore, to find the source of production of 15-HETE, quiescent HRMVECs were exposed to hypoxia for 30 minutes in the presence of 10 μCi [^{3}H]-AA and 10 μM calcium ionophore A23187, and the eicosanoids released into the medium were

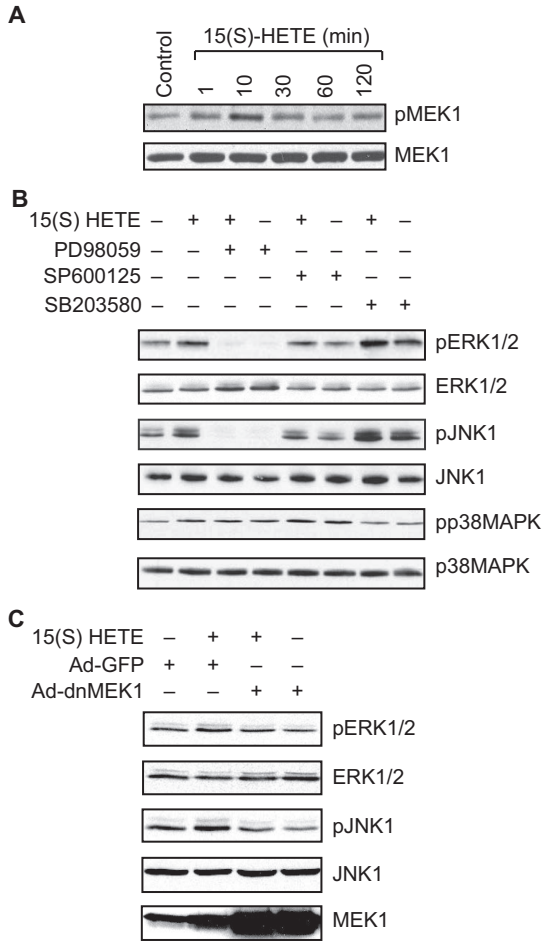

Figure 6. Effects of PD98059, SP600125, SB203580, and dnMEK-1 on 15(S)-HETE–induced phosphorylation of ERK1/2, JNK1, and p38 MAPK in HRMVECs. (**A**) Quiescent HRMVECs were treated with vehicle or 0.1 μM 15(S)-HETE for the indicated times, and cell extracts were prepared. Equal amounts of protein from control and each treatment were analyzed by Western blotting for phosphorylated MEK1 levels using its phosphospecific antibodies. As a loading control, the same blot was reprobed with its normal antibodies. (**B**) Quiescent HRMVECs were treated with vehicle or 0.1 μM 15(S)-HETE in the presence and absence of PD98059 (30 μM), SP600125 (10 μM), or SB203580 (10 μM) for 10 minutes, and cell extracts were prepared. Equal amounts of protein from control and each treatment were analyzed by Western blotting for phosphorylated ERK1/2, JNK1, and p38 MAPK levels using their phosphospecific antibodies. As a loading control, the same blots were reprobed with their respective normal antibodies. (**C**) HRMVECs were infected with either Ad-GFP or Ad-dnMEK1 at an MOI of 80, underwent quiescence, and were treated with vehicle or 0.1 μM 15(S)-HETE for 10 minutes, and cell extracts were prepared and analyzed for phosphorylated ERK1/2 and JNK1 levels, as described in (**B**).

extracted and analyzed by reverse-phase HPLC. The eluate of the peak, with a retention time of 50 minutes, was collected and subjected to chiral-phase HPLC. The chiral-phase HPLC analysis of 50-minute reverse-phase HPLC fractions indicated the presence of 15(S)-HETE to a major level (90%) and 15(R)-HETE to a minor level (10%; Fig. 2B). This result confirms the enzymatic production of 15(S)-HETE by HRMVECs in response to hypoxia. To understand the potential role of the 15-LOX1 to 15(S)-HETE axis in hypoxia-induced angiogenesis, we studied the effect of NDGA on hypoxia-induced HRMVEC migration and tube formation. As shown in Figure 2C-E, NDGA inhibited hypoxia-induced HRMVEC migration and tube formation.

To understand the relationship between HETEs and retinal neovascularization, we next tested the effect of 5(S)-HETE, 12(S)-HETE, and 15(S)-HETE on HRMVEC migration and tube formation under normoxia. Among these three HETEs, only 15(S)-HETE increased HRMVEC migration to a significant level (threefold vs. control). Furthermore, the chemotactic effect of 15(S)-HETE was higher than that caused by 20 ng/mL FGF-2 (Fig. 3A). Although all three HETEs induced HRMVEC tube formation, the effect of 12(S)- and 15(S)-HETEs was slightly higher than that of 5(S)-HETE and equal to that of 20 ng/mL FGF-2 (Fig. 3B).

Because human neonatal vessels and HRMVECs produced higher levels of 15(S)-HETE under hypoxic than normoxic conditions, we next focused on the elucidation of mechanisms underlying its angiogenic effects. For these studies, we examined the role of extracellular signal-regulated kinases 1/2 (ERK1/2), Jun N-terminal kinase 1 (JNK1), and p38 mitogen-activated protein kinase (p38 MAPK) groups of MAPKs. Western blot analysis of an equal amount of protein from control and various times of 15(S)-HETE–treated HRMVECs showed a time-dependent increase in the phosphorylation of ERK1/2, JNK1, and p38 MAPK (Fig. 4). A biphasic increase in the phosphorylation of ERK1/2 was observed, with a first peak around 10 minutes after 15(S)-HETE treatment, followed by a second peak at 2 hours. Peak phosphorylation of JNK1 occurred at 10 minutes, followed by a decrease at 30 minutes and a gradual increase thereafter. On the other hand, the phosphorylation of p38 MAPK was increased at 30 minutes, and this effect was sustained for at least 2 hours (Fig. 4). PD98059, a potent inhibitor of MEK1/2,[38] at a concentration of 30 μM completely suppressed 15(S)-HETE–induced HRMVEC migration and tube formation. Similarly, SP600125, a potent and specific inhibitor of JNK,[39] also blocked 15(S)-HETE–induced HRMVEC migration and tube formation. In contrast, SB203580, a potent inhibitor of p38 MAPK,[40] attenuated 15(S)-HETE–induced migration only but had no effect on tube formation (Figs. 5A–C). Interestingly, only PD98059 and SP600125, but not SB203580, inhibited 15(S)-HETE–induced basement membrane matrix (Matrigel: BD Biosciences) plug angiogenesis (Fig. 5D).

To test whether 15(S)-HETE stimulates ERK1/2 and JNK1 through a common mechanism, we next studied the role of MEK1 and found that 15(S)-HETE stimulated MEK1 phosphorylation in a time-dependent manner, with a maximum increase at 10 minutes (Fig. 6A). PD98059, an inhibitor of MEK1/2,

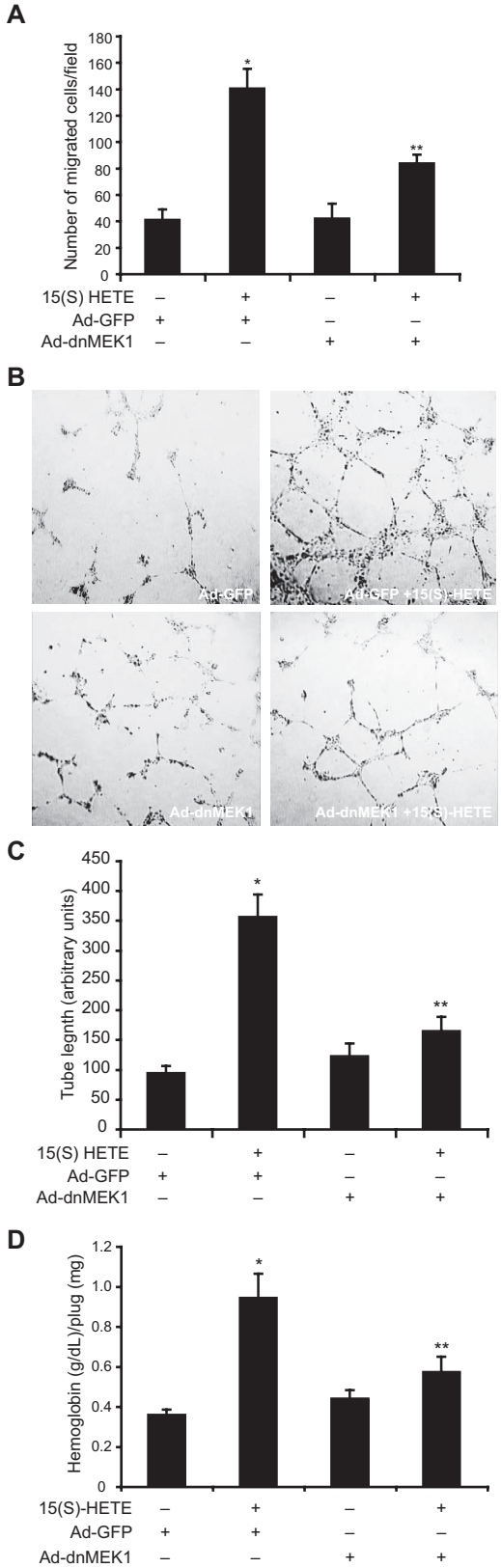

FIGURE 7. Adenoviral-mediated expression of dominant-negative MEK1 suppresses 15(S)-HETE–induced HRMVEC migration and tube formation and basement membrane matrix plug angiogenesis. HRMVECs were infected with Ad-GFP or Ad-dnMEK1 at an MOI of 80, underwent quiescence, and were subjected to vehicle or 0.1 μM of 15(S)-HETE–induced migration (**A**) and tube formation (**B**, **C**) as described in the Figure 3 legend. (**D**) C57BL/6 mice were injected subcutaneously with 0.5 mL basement membrane matrix premixed with vehicle or 50 μM 15(S)-HETE, with and without adenovirus expressing either GFP (1×10^8 pfu) or dnMEK1 (1×10^8 pfu). One week later, the animals were killed, and the basement membrane matrix plugs were harvested from under the skin and were analyzed for hemoglobin with Drabkin reagent. Values are the mean ± SD of three independent experiments or four animals. $^*P < 0.01$ versus control. $^{**}P < 0.01$ versus 15(S)-HETE treatment alone.

blocked ERK1/2 phosphorylation and attenuated JNK1 phosphorylation but had no effect on p38 MAPK phosphorylation induced by 15(S)-HETE (Fig. 6B). PD98059 by itself enhanced the basal phosphorylation of p38 MAPK. SP600125 inhibited 15(S)-HETE–induced JNK1 phosphorylation but either had no effect or enhanced the phosphorylation of ERK1/2 and p38 MAPK. On the other hand, SB203580 suppressed the phosphorylation of p38 MAPK only. These results strongly suggest that both ERK1/2 and JNK1 are activated by MEK1/2 in response to 15(S)-HETE.

To substantiate this finding further, we tested the effect of dnMEK1. Adenovirus-mediated expression of dnMEK1 completely blocked ERK1/2 and JNK1 phosphorylation induced by 15(S)-HETE (Fig. 6C). To understand the role of MEK1 in 15(S)-HETE–induced angiogenesis, we tested the effect of dnMEK1 on HRMVEC migration, tube formation, and basement membrane matrix (Matrigel; BD Biosciences) plug angiogenesis. Adenovirus-mediated expression of dnMEK1 suppressed all of them (Figs. 7A–D).

Discussion

The present study yielded several important findings. HRMVECs expressed both 15-LOX1 and 15-LOX2. Hypoxia induced the expression of 15-LOX1 and the production of its arachidonic acid metabolites 15(S)- and 12(S)-HETEs. 15(S)-HETE stimulated HRMVEC migration and tube formation as potently as 20 ng/mL of FGF-2. 15(S)-HETE stimulated ERK1/2, JNK1, and p38 MAPK phosphorylation in a time-dependent manner in HRMVECs. 15(S)-HETE–induced HRMVEC migration and tube formation, and basement membrane matrix (Matrigel; BD Biosciences) plug angiogenesis required ERK1/2 and JNK1 activation. 15(S)-HETE stimulated MEK1 phosphorylation in a time-dependent manner in HRMVECs. Inhibition of MEK1 by pharmacologic treatments or transduction of its dominant-negative mutant suppressed the 15(S)-HETE–induced ERK1/2 and JNK1 phosphorylation in HRMVECs and the migration and tube formation of these cells as well as basement membrane matrix (Matrigel; BD Biosciences) plug angiogenesis.

Evidence indicates that 15-LOX1 and 15-LOX2 play opposite roles in the regulation of cell growth; the latter is predominantly associated with proapoptotic signaling.[17,18,23–26] Similarly, 15(S)-HETE, which could be produced by the actions of these enzymes on arachidonic acid, plays a role in the regulation of cell growth and apoptosis.[16,41,42] It was demonstrated that human neonatal vessels, on exposure to hypoxia, produce hydroxyacids, including 15(S)-HETE.[29] In addition, 15(S)-HETE enhances HRMVEC migration.[28] The present finding that the expression of 15-LOX1 is induced by hypoxia in HRMVECs, resulting in the production of 15(S)-HETE, implies that 15-LOX1–15(S)-HETE signaling is involved in the angiogenic differentiation of these cells. This assumption was further supported by the observation that 15(S)-HETE is the most potent of the three HETEs tested in the stimulation of HRMVEC migration and tube formation, and it was as effective as 20 ng/mL FGF-2 in inducing these angiogenic events in HRMVECs. Given that exposure of human neonatal vessels to hypoxia led to increased production of 15(S)-HETE and that it has the ability to stimulate angiogenesis,[43] it is possible that this eicosanoid may be involved in the pathogenesis of retinal neovascularization. Because 15-LOX1 also converts arachidonic acid to 12(S)-HETE and this eicosanoid is produced in HRMVECs in response to hypoxia, a role for 12(S)-HETE in retinal neovascularization cannot be ruled out. In fact, it was demonstrated that 12(S)-HETE induces angiogenesis and prostate tumor growth.[44]

Previously, we have shown that arachidonic acid stimulates ERK1/2, JNK1, and p38 MAPK in vascular smooth muscle cells (VSMCs), responses that require its conversion through the LOX pathway.[33,45,46] Furthermore, arachidonic acid–induced VSMC migration required activation of ERKs, JNKs, and p38 MAPK.[46] In this study, we showed that 15(S)-HETE stimulates all three major groups of MAPKs—ERK1/2, JNK1, and p38 MAPK—in HRMVECs. Although a role for all three major groups of MAPKs in the regulation of cell migration has been demonstrated[47–50] and 15(S)-HETE–induced HRMVECs migration appeared to be dependent on the activation of ERK1/2, JNK1, and p38 MAPK, only the former two groups of MAPKs seemed to be involved in angiogenesis induced by this lipid molecule. Other studies have shown that ERKs and JNKs played roles in angiogenesis.[51]

A large body of data suggests that MEK1/2 (also known as MKK1/2) plays a role in the activation of ERK1/2.[48] Similarly, MKK4/7 and MKK3/6 have been reported to be involved in the phosphorylation and activation of JNKs and p38 MAPK, respectively.[52] It is interesting to note that 15(S)-HETE–induced ERK1/2 and JNK1 phosphorylation in HRMVECs is mediated by MEK1. Furthermore, blocking MEK1 activation by pharmacologic treatments or transduction of its dominant-negative mutant inhibited 15(S)-HETE–induced HRMVEC migration, tube formation, and basement membrane matrix (Matrigel; BD Biosciences) plug angiogenesis. Based on these observations, it is possible that MEK1 mediates 15(S)-HETE–induced HRMVEC angiogenic events by targeting both ERK1/2 and JNK1. A role for MAPK in serine phosphorylation and activation of STATs, particularly STAT-1 and STAT-3, has been demonstrated.[53] Recently, we have shown that STAT-3 is involved in 15(S)-HETE–induced VEGF expression and angiogenesis.[54] Based on these observations, it is possible that MEK1, by targeting ERK1/2 and JNK1, may facilitate serine phosphorylation and activation of STAT-3, leading to VEGF expression and angiogenesis. Further studies are required to address whether this is the mechanism involved in 15(S)-HETE–induced retinal angiogenesis.

References

1. Folkman J, Shing Y. Angiogenesis. *J Biol Chem*. 1992;267:10931–10934.
2. Folkman J. Angiogenesis in cancer, vascular, rheumatoid and other disease. *Nat Med*. 1995;1:27–31.
3. Duda DG. Antiangiogenesis and drug delivery to tumors: bench to bedside and back. *Cancer Res*. 2006;66:3967–3970.
4. Khurana R, Simons M, Martin JF, Zachary IC. Role of angiogenesis in cardiovascular disease: a critical appraisal. *Circulation*. 2005; 112:1813–1824.
5. Winter PM, Morawski AM, Caruthers SD, et al. Molecular imaging of angiogenesis in early-stage atherosclerosis with alpha (v) beta3-integrin-targeted nanoparticles. *Circulation*. 2003;108:2270–2274.
6. Gariano RF, Gardner TW. Retinal angiogenesis in development and disease. *Nature*. 2005;438:960–966.
7. Campochiaro PA. Retinal and choroidal neovascularization. *J Cell Physiol*. 2000;184:301–310.
8. Winn HR, Rubio R, Berne RM. Brain adenosine concentration during hypoxia in rats. *Am J Physiol*. 1981;241:H235–H242.
9. Adair TH. Growth regulation of the vascular system: an emerging role for adenosine. *Am J Physiol*. 2005;289:R283–R296.
10. Frobert O, Haink G, Simonsen U, Gravholt CH, Levin M, Deussen A. Adenosine concentration in the porcine coronary artery wall and A_{2A} receptor involvement in hypoxia-induced vasodilation. *J Physiol*. 2006;570:375–384.
11. Hein TW, Xu W, Kuo L. Dilation of retinal arterioles in response to lactate: role of nitric oxide, guanylyl cyclase, and ATP-sensitive potassium channels. *Invest Ophthalmol Vis Sci*. 2006;47:693–699.
12. Shweiki D, Itin A, Soffer D, Keshet E. Vascular endothelial growth factor induced by hypoxia may mediate hypoxia-initiated angiogenesis. *Nature*. 1992;359:843–845.

13. Calvani M, Rapisarda A, Uranchimeg B, Shoemaker RH, Melillo G. Hypoxic induction of an HIF-1α-dependent bFGF autocrine loop drives angiogenesis in human endothelial cells. *Blood*. 2006;107: 2705–2712.
14. Yamada H, Yamada E, Ando A, et al. Platelet-derived growth factor A-induced retinal gliosis protects against ischemic retinopathy. *Am J Pathol*. 1999;156:477–487.
15. Kourembanas S, Hannan RL, Faller DV. Oxygen tension regulates the expression of the platelet-derived growth factor-B chain gene in human endothelial cells. *J Clin Invest*. 1990;86:670–674.
16. Postoak D, Nystuen L, King L, Ueno M, Beckman BS. 15-Lipoxygenase products of arachidonate play a role in proliferation of transformed eythroid cells. *Am J Physiol*. 1990;259:C849–C853.
17. Kelavkar UP, Nixon JB, Cohen C, Dillehay D, Eling TE, Badr KF. Overexpression of 15-lipoxygenase-1 in PC-3 human prostate cancer cells increases tumorigenesis. *Carcinogenesis*. 2001;22:1765–1773.
18. Kelavkar UP, Glasgow W, Olson SJ, Foster BA, Shappell SB. Overexpression of 12/15-lipoxygense, an artholog of human 15-lipoxygenase-1, in the prostate tumors of TRAMP mice. *Neoplasia*. 2004; 6:821–830.
19. Yla-Herttuala S, Rosenfeld ME, Parthasarthy S, et al. Colocalization of 15-lioxygenase mRNA and protein with epitopes of oxidized low density lipoprotein in macrophage-rich areas of atherosclerotic lesions. *Proc Natl Acad Asci USA*. 1990;87:6959–6963.
20. Gu JL, Pei H, Thomas L, et al. Ribozyme-mediated inhibition of rat leukocyte-type 12-lipoxygenase prevents intimal hyperplasia in balloon-injured rat carotid arteries. *Circulation*. 2001;103:1446–1452.
21. Liu B, Maher RJ, DeJonckheere JP, et al. 12(S)-HETE increases the motility of prostate tumor cells through selective activation of PKC alpha. *Adv Exp Med Biol*. 1997;400B:707–718.
22. Tang DG, Renaud C, Stojakovic S, Diglio CA, Porter A, Honn KV. 12(S)-HETE is a mitogenic factor for microvascular endothelial cells: its potential role in angiogenesis. *Biochem Biophys Res Commun*. 1995;211:462–468.
23. Hsi LC, Xi X, Lotan R, Shureiqi I, Lippman SM. The histone deacetylase inhibitor suberoylanilide hydroxamic acid induces apoptosis via induction of 15-lipoxygenase-1 in colorectal cancer cells. *Cancer Res*. 2004;64:8778–8781.
24. Shureiqi I, Jiang W, Zuo X, et al. The 15-lipoxygenase-1 product 13-S-hydroxyoctadecadienoic acid down-regulates PPAR-delta to induce apoptosis in colorectal cancer cells. *Proc Natl Acad Sci USA*. 2003;100:9968–9973.
25. Hsi LC, Wison LC, Eling TE. Opposing effects of 15-lipoxygease-1 and -2 metabolites on MAPK signaling in prostate: alteration in peroxisome proliferators-activated receptor gamma. *J Biol Chem*. 2002;277:40549–40556.
26. Bhatia B, Maldonado CJ, Tang S, et al. Subcellular localization and tumor-suppressive functions of 15-lipoxygenase 2 (15-LOX2) and its splice variants. *J Biol Chem*. 2003;278:25091–25100.
27. Brash AR, Boeglin WE, Chang MS. Discovery of a second 15(S)-lipoxygenase in humans. *Proc Natl Acad Sci USA*. 1997;94:6148–6152.
28. Graeber JE, Glaser BM, Setty BN, Jordan JA, Walenga RW, Stuart MJ. 15-Hydroxyeicosatetraenoic acid stimulates migration of human retinal microvessel endothelium in vitro and neovascularization in vivo. *Prostaglandins*. 1990;39:665–673.
29. Setty BN, Ganley C, Stuart MJ. Effect of changes in oxygen tension on vascular and platelet hydroxyacid metabolites, II: hypoxia increases 15-hydroxyeicosatetraenoic acid, a proangiogenic metabolite. *Pediatrics*. 1985;75:911–915.
30. Mansour SJ, Matten WT, Hermann AS, et al. Transformation of mammalian cells by constitutively active MAP kinase kinase. *Science*. 1994;265:966–970.
31. Liu Z, Zhang C, Dronadula N, Li Q, Rao GN. Blockade of nuclear factor of activated T cells activation signaling suppresses balloon injury-induced neointima formation in a rat carotid artery model. *J Biol Chem*. 2005;280:14700–14708.
32. Berkner KL. Development of adenovirus vectors for the expression of heterologous genes. *Biotechniques*. 1988;6:616–629.
33. Rao GN, Baas AS, Glasgow WC, Eling TE, Runge MS, Alexander RW. Activation of mitogen-activated protein kinases by arachidonic acid and its metabolites in vascular smooth muscle cells. *J Biol Chem*. 1994;269:32586–32591.
34. Nony PA, Kennett SB, Glasgow WC, Olden K, Roberts JD. 15(S)-Lipoxygenase-2 mediates arachidonic acid-stimulated adhesion of human breast carcinoma cells through the activation of TAK1, MKK6, and p38 MAPK. *J Biol Chem*. 2005;280:31413–31419.
35. Nagata D, Mogi M, Walsh K. AMP-activated protein kinase (AMPK) signaling in endothelial cells is essential for angiogenesis in response to hypoxic stress. *J Biol Chem*. 2003;278: 31000–31006.
36. Medhora M, Daniels J, Mundey K, et al. Epoxygenase-driven angiogenesis in human lung microvascular endothelial cells. *Am J Physiol*. 2003;284:H215–H224.
37. Orning L, Hammarstrom S. Inhibition of leukotriene C and leukotriene D biosynthesis. *J Biol Chem*. 1980;255:8023–8026.
38. Alessi DR, Cuenda A, Cohen P, Dudley DT, Saltiel AR. PD 098059 is a specific inhibitor of the activation of mitogen-activated protein kinase kinase in vitro and in vivo. *J Biol Chem*. 1995;270:27489–27494.
39. Lee JC, Laydon JT, McDonnell PC, et al. A protein kinase involved in the regulation of inflammatory cytokine biosynthesis. *Nature*. 1994;372:739–746.
40. Bennett BL, Sasaki DT, Murray BW, et al. SP600125, an anthrapyrazolone inhibitor of Jun N-terminal kinase. *Proc Natl Acad Sci USA*. 2001;98:13681–13686.
41. Setty BN, Graeber JE, Stuart MJ. The mitogenic effect of 15- and 12-hydroxyeicosatetraenoic acid on endothelial cells may be mediated via diacylglycerol kinase inhibition. *J Biol Chem*. 1987;262: 17613–17622.
42. Chang MS, Schneider C, Roberts RL, et al. Detection and subcellular localization of two 15S-lipoxygenases in human cornea. *Invest Ophthalmol Vis Sci*. 2005;46:849–856.
43. Zhang B, Cao H, Rao GN. 15(S)-Hydroxyeicosatetraenoic acid induces angiogenesis via activation of PI3K-Akt-mTOR-S6K1 signaling. *Cancer Res*. 2005;65:7283–7291.
44. Nie D, Krishnamoorthy S, Jin R, et al. Mechanisms of regulating tumor angiogenesis by 12-lipoxygenase in prostate cancer cells. *J Biol Chem*. 2006;281:18601–18609.
45. Madamanchi NR, Bukoski RD, Runge MS, Rao GN. Arachidonic acid activates Jun N-terminal kinase in vascular smooth muscle cells. *Oncogene*. 1998;16:417–422.
46. Dronadula N, Rizvi F, Blaskova E, Li Q, Rao GN. Involvement of cAMP-response element binding protein-1 in arachidonic acid-induced vascular smooth muscle cell motility. *J Lipid Res*. 2006; 47:767–777.
47. Huang C, Jacobson K, Schaller MD. MAP kinases and cell migration. *J Cell Sci*. 2004;117:4619–4628.
48. Matsubayashi Y, Ebisuya M, Honjoh S, Nishida E. ERK activation propagates in epithelial cell sheets and regulates their migration during wound healing. *Curr Biol*. 2004;4:731–735.
49. Frey MR, Golovin A, Polk DB. Epidermal growth factor-stimulated intestinal epithelial cell migration requires Src family kinase-dependent p38 MAPK signaling. *J Biol Chem*. 2004;279: 44513–44521.
50. Miyamoto Y, Yamauchi J, Mizuno N, Itoh H. The adaptor protein Nck1 mediates endothelin A receptor-regulated cell migration through the Cdc42-dependent c-Jun N-terminal kinase pathway. *J Biol Chem*. 2004;279:34336–34342.
51. Salameh A, Galvagni F, Bardelli M, Bussolino F, Oliviero S. Direct recruitment of CRK and GRB2 to VEGFR-3 induces proliferation, migration, and survival of endothelial cells through the activation of ERK, AKT, and JNK pathways. *Blood*. 2005; 106:3423–3431.
52. Davis RJ. Signal transduction by the JNK group of MAP kinases. *Cell*. 2000;103:239–252.
53. Stephens JM, Lumpkin SJ, Fishman JB. Activation of signal transducers and activators of transcription 1 and 3 by leukemia inhibitory factor, oncostatin-M, and interferon-γ in adipocytes. *J Biol Chem*. 1998;273:31408–31416.
54. Srivastava K, Kundumani-Sridharan V, Zhang B, Bajpai AK, Rao GN. 15(S)-Hydroxyeicosatetraenoic acid-induced angiogenesis requires signal transducer and activator of transcription-3-dependent expression of vascular endothelial growth factor. *Cancer Res*. 2007; 67:4328–4336.